Chapter 9
Determining Ocean Circulation and Sea Level from Satellite Altimetry: Progress and Challenges

Lee-Lueng Fu

9.1 Introduction

The idea of flying a radar altimeter in space to measure the height of sea surface for a variety of geophysical studies was quickly developed after the first launch of artificial satellite. Seasat, launched in 1978, carried the first radar altimeter with a precision capable of revealing the variability of ocean currents. After the premature demise of the mission after only 3 months' data collection, the oceanographic community realized the potential of satellite altimetry for making global observation of the ocean. The military community also realized the utility of the measurement for naval operations and hence launched Geosat in 1985. The instrument itself was a copy of Seasat, but without the correction for the effects of tropospheric water vapor due to the lack of an onboard radiometer. The oceanographic community was more ambitious in developing a mission specifically designed for studying the ocean circulation and its variability, leading to the Franco-American collaboration in the TOPEX/Poseidon Mission (T/P), launched in 1992.

While T/P was in development, the data from Geosat, although not as accurate as oceanographers had desired, provided nonetheless the first multi-year altimetry data for the study of ocean dynamics as well as a test bed for processing altimetry data. As part of the payload of the European Remote Sensing satellite (ERS-1), a radar altimeter similar to Seasat was launched by the European Space Agency (ESA) in 1991. The launch of T/P then started an era in which at least two satellite altimeters were flying simultaneously. The era has continued as of the writing of the article today. Results from these missions cover a wide range of earth sciences: oceanography, geophysics, geodesy, and hydrology. Fu and Cazenave (2001) provided a comprehensive review. There has been tremendous progress made since that review. The scope of this paper, however, is focused on recent progress in the study of ocean circulation and sea level change, including some recap of earlier results to provide a historic perspective. At the end, the limitation of the present approach and the challenges for future development are addressed.

L.-L. Fu (✉)
Jet Propulsion Laboratory, California Institute of Technology, Pasadena, CA 91109-8099, USA
e-mail: lee-lueng.fu@jpl.nasa.gov

V. Barale et al. (eds.), *Oceanography from Space*,
DOI 10.1007/978-90-481-8681-5_9,

9.2 Ocean General Circulation

A major driving goal for developing ocean altimetry mission was the vision of determining the ocean general circulation from space (Wunsch and Gaposchkin, 1980). In parallel to the development of T/P, a satellite gravity mission was also conceived in the early 1980s for mapping the geoid, which in combination with altimetry measurement would yield the ocean circulation. The gravity mission did not materialize until the launch of the GRACE Mission in 2002. The accuracy of the GRACE geoid is estimated to be 2–3 mm at scales as small as 400 km (Tapley et al., 2004). This represents more than an order of magnitude improvement over the results based on previous geoid models, which have errors on the order of 10 cm at scales larger than 1,000 km (Fu and Chelton, 2001).

Most of the swift boundary currents in the ocean have cross-stream scales less than 100 km and thus are not fully resolved by using the GRACE geoid. As part of the World Ocean Circulation Experiment conducted in the 1990s, thousands of surface drifters were deployed in the ocean to measure surface current velocity. Such drifters suffer from sampling errors for computing the time mean velocity. This problem has been mitigated by combining the densely populated altimetry data with the drifter data to correct for the sampling bias in the latter. Using this technique, the surface mean circulation was estimated based on decade-long observations (Niiler et al., 2003; Rio and Hernandez, 2004). Many more details of the mean circulation have been revealed down to scales of 50–100 km. The spatial resolution is highly heterogeneous due to the drifters' uneven distribution. The most interesting finding is the prominent zonal striations in the surface mean circulation (Maximenko et al., 2005, 2008; see Fig. 9.1). The appearance of the striations was enhanced by applying a two-dimensional high-pass filter to the mean ocean dynamic topography.

Simulations by high-resolution ocean general circulation models (Richards et al., 2006) have shown similar features but the details (exact locations, orientations,

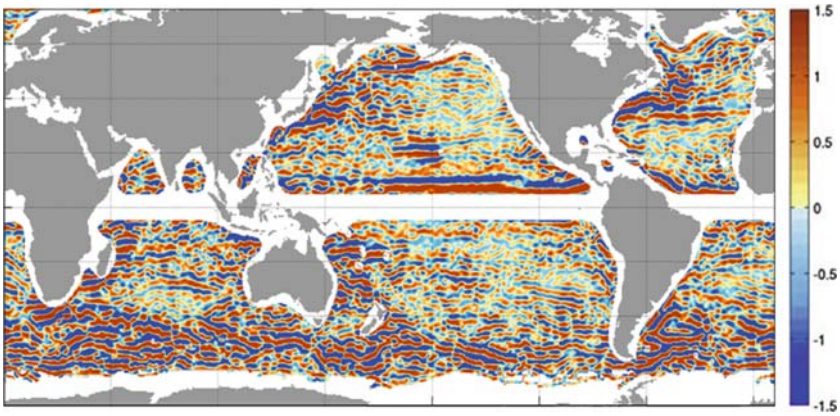

Fig. 9.1 1993–2002 mean zonal surface geostrophic velocity [cm/s] from drifter/altimetry based mean dynamic topography high-pass filtered with a two-dimensional Hanning filter of 4° half-width (from Maximenko et al., 2008)

strengths, etc.) exhibit discrepancies. The dynamic mechanisms for the striations are not yet well understood. Using a kinematic model of randomly distributed field of eddies, Schlax and Chelton (2008) showed that such striations could be caused by the migration of eddies that were not completely averaged out over a finite time period. The residual speed of the eddy currents after 10-year averaging is on the order of 1 cm/s, comparable to the results of Maximenko et al. (2008). As the residual currents go down with 1/T, where T is the averaging time, a data set of multiple decades is needed to average out the eddy effects.

A testimony of the quality of the surface mean dynamic topography of Niiler et al. (2003) was the study of the vorticity balance of the Antarctic Circumpolar Current (ACC) by Hughes (2005). Estimating the vorticity of the flow by differentiating the dynamic topography, Hughes (2005) discovered two modes of flow behaviors: Meanders in which a balance was achieved between the advection of relative and planetary vorticity as in a stationary equivalent-barotropic Rossby wave, and a flow in which the advection of total vorticity was related to bottom topographic steering.

9.3 Large Scale Low Frequency Variability

A series of El Niño Southern Oscillation events in the 1990s including the phenomenal event of 1997–1998 provided a focus for demonstrating the power of satellite altimetry to study large-scale climate variability. Fu and Smith (1996) demonstrated an early comparison of altimetry observation with a model simulation of a Pacific warming event. The success of satellite altimetry in providing global ocean observations was a major motivation for the advancement in global ocean modeling and data assimilation in the 1990s (Stammer et al., 1996, 2002). This development has establish a new framework for performing ocean reanalysis using modern state estimation approach by integrating data from a observing network into ocean general circulation models (Wunsch et al., 2009).

As the altimetry data record extended into its second decade, oceanographers for the first time had a continuous global data set for studying ocean variability beyond the seasonal-to-interannual scales. Hakkinen and Rhines (2004) reported a slow-down of the subpolar gyre circulation of the North Atlantic Ocean from analysis of T/P data in combination with earlier altimeter data. They attributed this change to weakened thermohaline forcing. Based on satellite altimetry data in combination with a variety of in-situ observations, Roemmich et al. (2007) discovered a decadal intensification of the subtropical gyre of the South Pacific Ocean from 1993 to 2004. The gyre circulation increased by 20%, resulting from a decadal strengthening of wind forcing east of New Zealand as part of a circumpolar change of climatic state. On the other hand, Lee (2004) found that the upper ocean overturning circulation of the Indian Ocean decreased by 70% from 1992 to 2000, caused by the weakening of the trade winds. Subsequently Lee and McPhaden (2008) found a larger-scale linkage of the decadal variability of the Indian and Pacific Oceans.

In the Pacific Ocean, sea surface temperature, wind stress, and ocean circulation are involved in a decadal variability called the Pacific Decadal Oscillation (PDO). Qiu and Chen (2009) analyzed 16 years' worth of altimetry data and noted that the phase transition of PDO triggered westward baroclinic Rossby waves, which affected the stability of the Kuroshio Extension upon arrival in that region. Shifting between stable and unstable regimes, the eddy energy and its interaction with the Kuroshio Extension is linked to the larger-scale PDO.

Westward propagation of large scale variability is a ubiquitous phenomenon well documented by numerous papers since the seminal paper by Chelton and Schlax (1996). Fu and Chelton (2001) provided a review of the subject. The conclusion then was that the predominant westward propagation was associated with baroclinic Rossby waves (see the Chapter 12 by Cipollini et al., this volume). Fu (2004) discussed the latitudinal variation of the frequency content of the propagation and identified cases in which the wave frequency was higher than allowed by the conventional Rossby wave theory. Some of the cases were attributable to barotropic Rossby waves.

9.4 Large Scale High Frequency Variability

A big surprise when the T/P data were first analyzed was the presence of large-scale variability of the ocean at periods on the order of 10 days. These turned out to be barotropic response of the ocean to rapid changes in wind forcing. Chao and Fu (1995) showed that the observed variability could be simulated by ocean general circulation models. The results were further confirmed by Fu and Smith (1996). A modeling study by Fukumori et al. (1998) suggested that up to 50% of the variance of such large-scale variability could have periods shorter than 20 days, the Nyquist period of T/P. This raised concerns for aliasing these high-frequency signals to low frequencies in altimetry data. Model simulations forced by good quality wind were then used to de-alias the high-frequency signals in altimetry data (e.g., Stammer et al., 2000; Carrere and Lyard, 2003).

To a large extent the high-frequency variability is influenced by bottom topography. Fu et al. (2001) found a 25-day oscillation of the Argentine Basin over the Zapiola Rise and explained it as a free barotropic mode of the basin (also see Weijer et al., 2007). Using a simple wind-driven linear vorticity model, Fu (2003) illustrated the intraseasonal variability of the Southern Ocean and the North Pacific Ocean could be explained as a balance between wind stress curl and relative vorticity with bottom friction. In the Indian Ocean, the highly periodic monsoon wind generates intraseasonal variability at periods of 180, 120, 90, 75 days (Fu, 2007). Some of these could be explained as resonant basin modes.

9.5 Mesoscale Eddies

Mesoscale variability was observed even by the GEOS-3 altimeter (Huang et al., 1978) with a noise level of 25 cm. The strength of the signals and the relatively

small scales made them survive the substantial instrument noise and orbit errors of the GEOS-3 altimeter. However, the trade-off between temporal and spatial resolution of a single altimeter has made it difficult to map the two-dimensional evolution of mesoscale eddies. Despite this difficulty, many statistical properties of mesoscale variability were ascertained from altimetry: geographic distribution of energy, spatial and temporal scales, wavenumber-frequency spectrum, eddy transports, viscosity and diffusivity (see Le Traon and Morrow, 2000 for a review).

The merging of multiple altimeter data into a gridded data set (Ducet et al., 2000) created a first opportunity to study the two-dimensional movement of mesoscale eddies. The intrinsic resolution of the data set is about 150–200 km, allowing to map eddies of sizes larger than these scales. The data set has created a surge of effort in tracking eddies, e.g. off the Central America coast (Palacios and Bograd, 2005) and in the Oyashio (Isoguchi and Kawamura, 2006) and studying their behavior. Advanced methods exist for tracking certain vorticity properties of eddies and allow automatic tracking (Isern-Fontanet et al., 2006; Morrow et al., 2004; Chelton et al., 2007). Figure 9.2 summarizes the properties of large eddies with lifetime grater 12 weeks surveyed by Chelton et al. (2007). A notable feature is that the propagation of cyclonic eddies has a slight tendency for a poleward deflection from purely westward. Anti-cyclonic eddies have a slight tendency for an equatorward deflection. At low latitudes, the westward speed of eddy propagation is somewhat less than that of non-dispersive baroclinic Rossby waves represented by the large-scale variability. At mid and high latitudes, the eddy speed is indistinguishable from the Rossby wave speed.

Using the maximum correlation method, Fu (2006, 2009) mapped the propagation velocity vector of ocean eddy variability. The method used the spatial and temporal lags of the maximum correlation of time series of sea surface height anomalies to compute the velocity of propagation of the dominant variability in the time series. The results correspond to the energy containing variability mostly associated with mesoscale motions, but cannot distinguish isolated eddies from other forms of variability like meandering currents and fronts. Displayed in Fig. 9.3 is an example in the Southern Ocean (from Fu, 2009), showing the vectors of propagation superimposed on the bottom topography (color shade) along with the tracks of the Subtropical Front, the Sub-Antarctic Front, and the Polar Front.

Within the Antarctic Circumpolar Current (ACC) which basically flows eastward parallel to these fronts, eddy propagation is steered from westward to eastward by the mean currents. A prominent feature is the "U" shaped turn of eddy propagation over a fracture zone centered at 55°S and 240°E (the Menard Fracture Zone). Another notable influence of bottom topography and ACC is the deflection of eddy paths over the Mid-Atlantic Ridge between 340° and 360°E. In the Argentine Basin, a counter-clockwise gyre-like pattern of eddy propagation is centered over a topographic feature called the Zapiola Rise. The center of the "gyre" seems to be a region where eddies tend to dissipate. This may be evidence for eddies being a source of energy driving the large-scale counter-clockwise (anti-cyclonic) barotropic circulation over the Zapiola Rise (de Miranda et al., 1999).

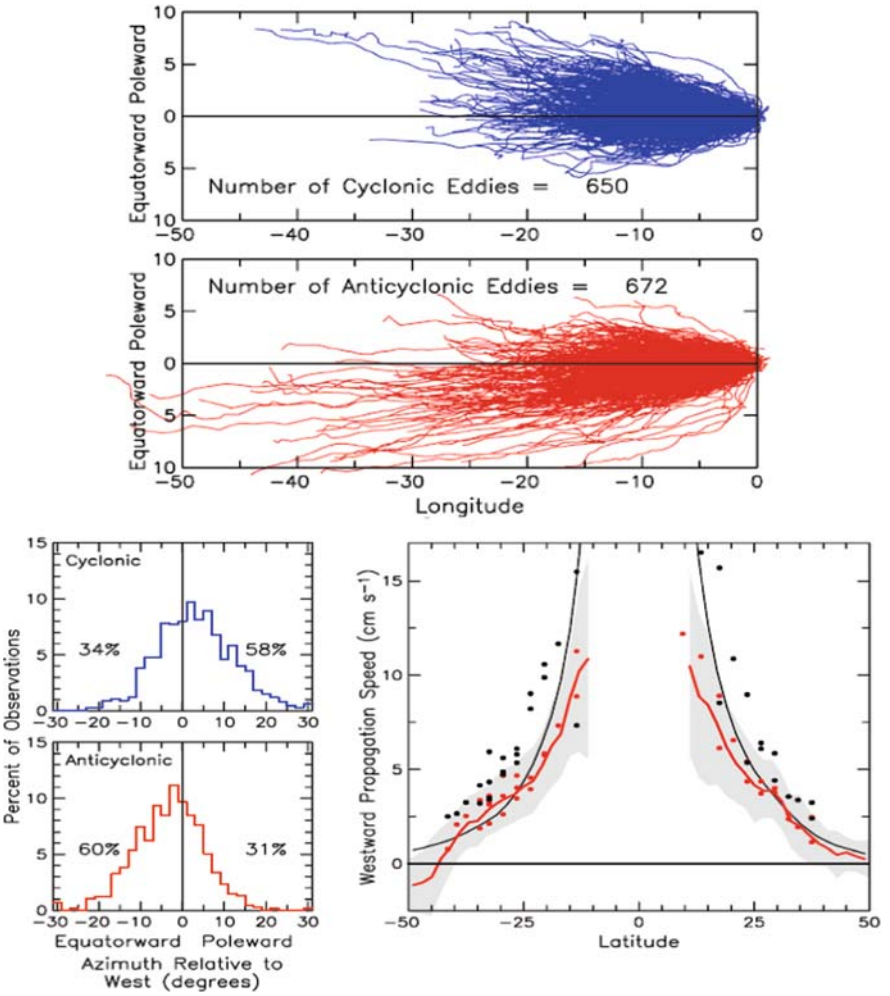

Fig. 9.2 The global propagation characteristics of long-lived cyclonic and anti-cyclonic eddies with lifetimes longer than 12 weeks. *Upper panels*: relative changes in longitude (negative westward) and latitude (poleward vs. equatorward). *Lower left panels*: histograms of the mean propagation angle relative to due west. *Lower right panel*: latitudinal variation of the westward zonal propagation speeds of large-scale sea surface height (*black dots*) and small-scale eddies (*red dots*) along the selected zonal sections considered previously by Chelton and Schlax (1996). The global zonal average of the propagation speeds is shown in the *right panel* by the *red line*, with *gray shading* to indicate the central 68% of the distribution in each latitude band, and the propagation speed of nondispersive baroclinic Rossby waves is shown by the *black line* (from Chelton et al., 2007)

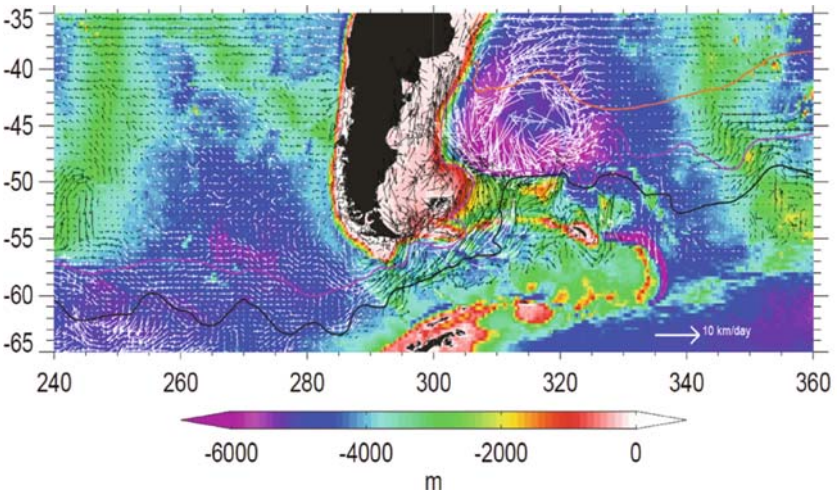

Fig. 9.3 The velocity of eddy propagation in the Southern Ocean between 240° and 360°E, superimposed on the ocean bathymetry. The different colors of the *arrows* are for the ease of viewing. The *three colored curves* are (from north to south) the Subtropical Front, the Sub-Antarctic Front, and the Polar Front, respectively (from Fu, 2009)

9.6 Energy Cascade and Eddy-Mean Flow Interaction

A fundamental issue in ocean dynamics is the flux of kinetic energy in wavenumber spectral space. Namely, the rate of energy transfer across different scales. Theoretical and modeling work suggests that baroclinic energy would cascade from high-order modes to the first mode, where the energy is transferred into barotropic mode, which then goes through an inverse cascade to larger scales (Rhines, 1977; Fu and Flierl, 1980). There was no direct observational evidence for the validity of these ideas until Scott and Wang (2005) computed the spectral energy flux directly using the gridded data set from merged multiple altimeter observations. As shown in Fig. 9.4, there is an inverse cascade of energy (negative flux) from the first baroclinic deformation scale to larger scales. Because altimetry observations are primarily related to the energy in the first baroclinic mode, this result indicates that the baroclinic energy in the ocean has an inverse cascade, in contrast to previous theoretical predictions.

Scott and Arbic (2007) then used a quasi-geostrophic model to illustrate that the inverse cascade is dominated by baroclinic modes in the model simulations. Altimetry observations have been used to revise a long-held theoretical concept about ocean dynamics. Using the same technique, Qiu et al. (2008) studied the seasonally modulated energy exchange process between the mean flow and eddy field of the Subtropical Counter Current in the South Pacific Ocean. They found a transfer of energy from meridionally-oriented modes to zonally-oriented modes through baroclinic instability. The energy is then transferred to larger zonal scales in an anisotropic inverse cascade process reflecting the effect of the meridionally changing Coriolis force (the beta effect). This is the first demonstration of the

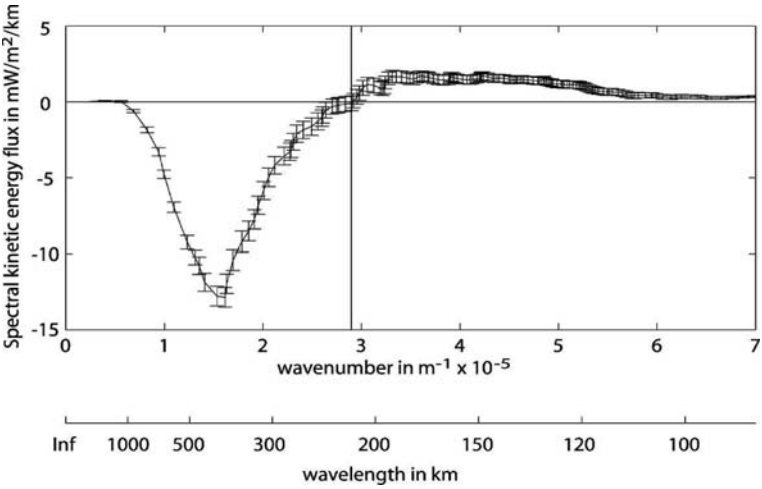

Fig. 9.4 The spectral kinetic energy flux associated with the near-surface geostrophic flow in the Kuroshio Extension region from altimeter data (∼ 24°–46°N, 156°–174°E). The *straight vertical line* indicates the wavenumber of the first baroclinic deformation scale averaged over the region (Scott and Arbic, 2007)

detailed mechanism of energy exchange between mean flow and eddy variability and the transformation of scales.

9.7 Tides

T/P was the only altimeter mission that was designed to fly in a orbit optimized for resolving tidal signals for separation from those of ocean circulation. This effort has led to the most accurate information of the barotropic tides in the open ocean (Le Provost, 2001). Using the tide models derived from T/P, Egbert and Ray (2000) computed the flux of tidal energy and concluded that up to 30% of the total tidal dissipation took place in the deep ocean, in contrast to the traditional notion that more than 90% of tidal dissipation occurred over the shelves and shallow seas. This finding has confirmed the conjecture of Munk and Wunsch (1998) that half of the energy (about one terawatt) required to mix the ocean waters to maintain the thermohaline circulation comes from the tidal dissipation in the deep ocean. A major mechanism for converting tidal energy to mixing energy is through scattering of barotropic tides into internal tides over rough topography. Ray and Mitchum (1997) demonstrated that surface manifestations of internal tides could be detected in altimetry data. This work has led to a surge of studies of ocean internal tides, their sources, pathways and energetics (e.g. Merrifield et al., 2001).

9.8 Global Sea Level Change

The ability of measuring the change of the global mean sea level with uncertainty on the order of 1 mm/year represents the culmination of the development of

precision altimetry. Although T/P and its follow-ons were not designed for meeting performance requirement at this level, through a dedicated effort of a large team of scientists and engineers, it has been demonstrated that the measurement accuracy has reached sub mm/year level (Ablain et al., 2009). The record of altimetry data from T/P and its follow-ons, supplemented by data from other missions, has provided the foundation for the determination of present-day sea level change (Cazenave and Nerem, 2004). The global coverage of altimetry observation has provided not only a mean value of the sea level rise, estimated at a rate of 3.4 $\pm$ 0.6 mm/year, from 1993 to 2008 (Ablain et al., 2009), but also a map of the geographical pattern of sea level change.

Shown in Fig. 9.5 is such a map (from Merrifield et al., 2009), which illustrates the complexity of the decadal variability of sea level as discussed in Section 9.3. Also shown are the locations of well-surveyed tide gauge locations. It is clear that tide gauges alone cannot capture the complicated geographic variability of sea level. As the planet is warming up, the potential threat of the collapse of polar ice sheets creates a geographically uneven risk of inundation (Bamber et al., 2009). It is therefore important to closely monitor not only the global mean sea level rise, but also its geographic pattern for early warnings and adaptations.

The launch of the GRACE satellite and the deployment of the Argo floats in the world's oceans, together with satellite altimetry, have provided an observing system for separating the contributions to sea level change into its components- the change of steric sea level and ocean mass. The three independent measurements allow a consistency check of the individual measurements. The total sea level can be determined by altimetry directly or by the combination of Argo with GRACE. The steric sea level can be determined by Argo directly or by the combination of

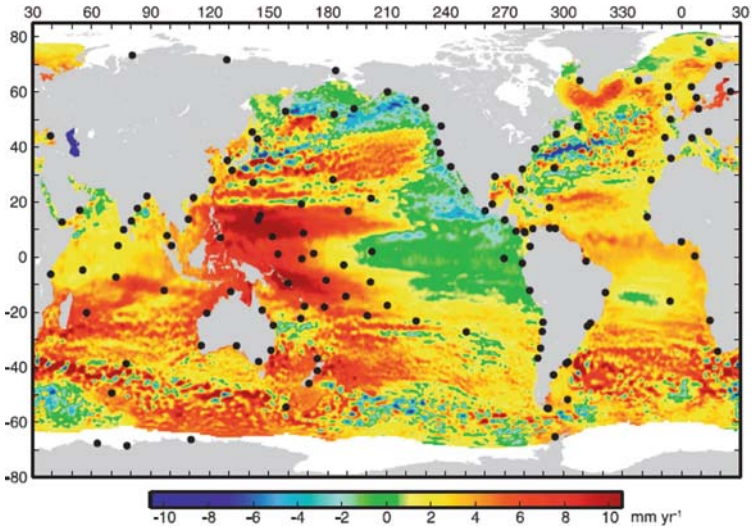

Fig. 9.5 Sea level trends (1993–2007) from multi-mission gridded sea level anomalies. The *black dots* are locations of well-surveyed tide gauges (from Merrifield et al., 2009)

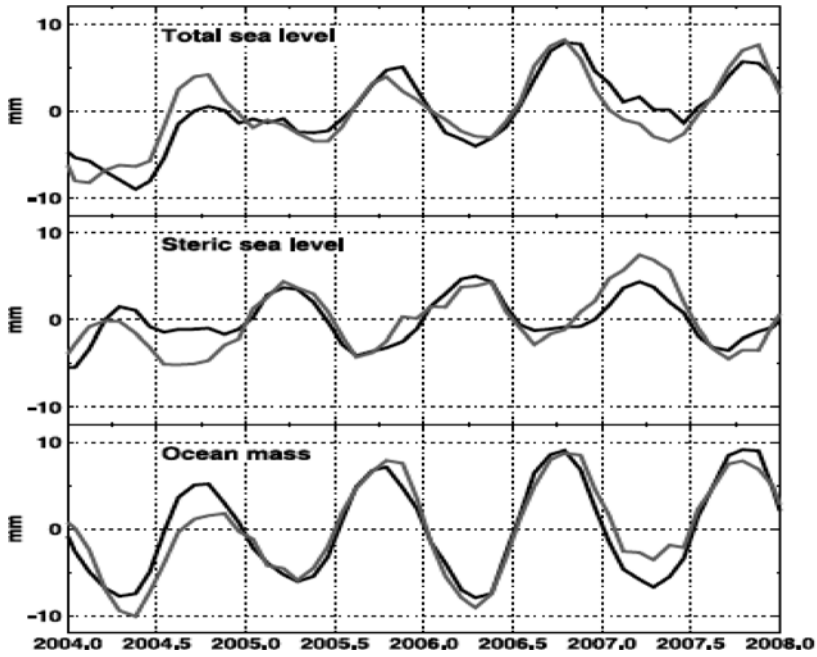

Fig. 9.6 Variability in total global mean sea level and its steric and mass components. The *black lines* are the observed (*top*) total sea level from Jason-1, (*middle*) steric sea level from Argo, and (*bottom*) ocean mass from GRACE. The *gray lines* show the inferred variability from the complementary observations. A 3-month boxcar smoothing is applied to each time series (from Leuliette and Miller, 2009)

altimetry and GRACE. The ocean mass can be determined directly by GRACE or by the combination of altimetry and Argo.

Figure 9.6 (from Leuliette and Miller, 2009) shows that the two estimates of each of the three components are consistent with each other to the extent of the errors of each. Maintaining the three measurement systems for monitoring and understanding future sea level change is crucial for preparing for the impact of a warming climate to our society.

9.9 Future Challenges

The sampling of a single altimeter presents a trade-off between spatial and temporal resolutions. Since the launch of T/P and ERS-1 in the early 1990s, it has been fortunate to have at least 2 altimeters fly simultaneously.

The spatial resolution of the merged data set from two altimeters is estimated to be from 150 km (Ducet et al., 2000) to 3° in longitude (Chelton and Schlax, 2003). This has prevented the observation of ocean variability smaller than these scales that contains a substantial amount of kinetic energy and plays significant roles in mixing and dissipation in the energy cycle of ocean circulation.

For example, Lapeyre and Klein (2006) illustrated that up to 50% of the oceanic tracer content is found at scales shorter than 100 km. Analyzing simulations by a high-resolution ocean general circulation model, Klein et al. (2009) showed that the vertical velocity of upper ocean currents can be estimated from sea surface height at the sub-mesoscales (wavelengths shorter than 100 km). Therefore, a significant part of ocean circulation and variability that has a fundamental role in the vertical exchange process for transporting nutrients, CO_2, and heat has been missed in the current altimetry observations.

To extend altimetry observation to higher resolution over a wide swath, radar interferometry has been developed since the early 1990s (Rodriguez and Martin, 1992). An instrument called Wide-Swath Ocean Altimeter (WSOA) was developed for flight on the Ocean Surface Topography Mission/Jason-2 in the early 2000s (Fu and Rodriguez, 2004).

Because of funding problems, WSOA was cancelled after substantial development had been conducted. A new mission concept called Surface Water and Ocean Topography (SWOT) was recommended by the US National Research Council Decadal Survey for addressing the need of high-resolution observation of water elevation in both the oceans and land surface water (Alsdorf et al., 2007). SWOT is currently being developed by NASA and CNES for flight in the late 2010s.

A challenge SWOT is facing is illustrated in Fig. 9.7 (from Fu and Ferrari, 2008). The wavenumber spectrum of sea surface height anomaly observed by the Jason-1 altimeter shows the domination of instrument noise at wavelengths shorter than

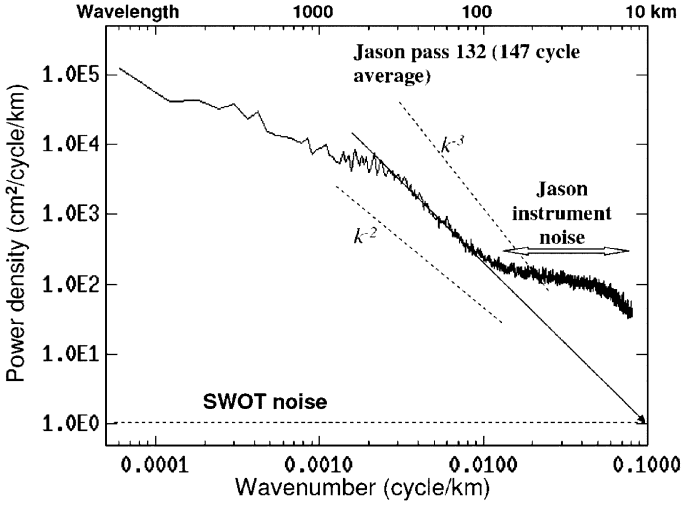

Fig. 9.7 Spectrum of sea surface height anomaly from Jason altimeter data (*solid line*). The *two slanted dashed lines* represent two spectral power laws with k as wavenumber. The *horizontal dashed line* represents the SWOT measurement noise at 1/km sampling rate. The *slanting solid straight line* represents a linear fit of the spectrum between 0.002 and 0.01 cycles/km. It intersects with the SWOT noise level at 10 km wavelength (from Fu and Ferrari, 2008)

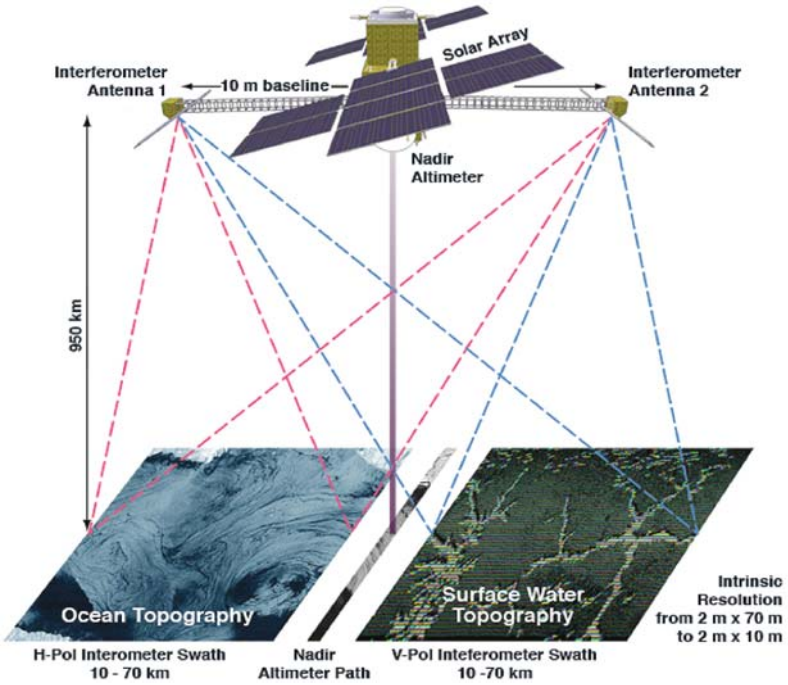

Fig. 9.8 The configuration of the SWOT[1] measurement system

100 km. Assuming that the spectrum of ocean signals continues to follow a power law extrapolation from the observation, the noise level of SWOT must be lower than that of Jason-1 by two orders of magnitude in order to resolve ocean signals down to a wavelength of 10 km.

Shown in Fig. 9.8 is the configuration of the SWOT measurement approach. The basic instrument payload is composed of two Ka-band synthetic aperture radars (SAR) with their antennae separated by a 10-m long mast. The intrinsic resolution of the SAR is on the order of a few meters to tens of meters. The backscatter of the ocean surface is received by the two antennae. Through the technique of interferometry and precision orbit determination, the height of the surface elevation of the backscatters can be determined. Using different polarizations, the two beams of radar transmission can be analyzed without interference. Over the ocean, the raw data are processed and smoothed onboard over cells of 1 km $\times$ 1 km to achieve the required low noise level. Over land, the raw data are transmitted to ground stations for processing according to the requirements for hydrological applications. The nadir track where interferometry does not work is to be covered by a conventional

[1] For more information on SWOT, see: http://bprc.osu.edu/water

nadir-looking Jason-class altimeter. The combined two swaths plus the nadir observation will provide a swath of width of 130 km for studying the mesoscale and submesoscale processes over the ocean and the storage and discharge of freshwater on land.

Because of the finite swath coverage, it takes at least 22 days to cover the Earth between the inclination latitudes without gaps. The repeat period of SWOT is set to 22 days. To avoid sun-synchronous orbits for sampling tides, the inclination of the orbit is set to 78°. At the oceanic mesoscales and submesoscales, shallow water tides and internal tides become key concerns for studying ocean circulation. These tides have not been well resolved by conventional altimetry and pose new challenges for SWOT. As noted in Section 9.7, tides in their own right are important to the understanding of ocean circulation. The choice of Ka-band for SWOT is primarily for meeting the interferometry measurement requirement because the height errors are proportional to the ratio of radar wavelength to the length of the mast. Furthermore, at Ka-band, the range delay caused by the ionospheric free electrons becomes negligible. To correct for the errors cause by the tropospheric water vapor, a multi-frequency microwave radiometer will be included in the payload.

9.10 Conclusions

Satellite altimetry has revolutionized oceanography since the 1990s. Precision missions like T/P and its follow-ons have provided the first view of large-scale ocean circulation, its variability, and the global mean sea level. The new observations have motivated the advancement in ocean modeling and data assimilation leading to the development of ocean state estimation for a variety of applications. The discovery of the high-frequency large-scale variability led to a new view and appreciation of the barotropic processes in the ocean. The decade-long data record provides the first global view of the decadal change in ocean circulation and its geographic variability. The capability of detecting the rate of global mean sea level change at a level of uncertainty less than 1 mm/year represents the state-of-the-art of precision altimetry. One must realize that T/P and its follow-ons were not designed for reaching this level of performance. The achievement was made by a dedicated effort of a large team of scientists and engineers to push the limit of the measurement system. While altimetry system is being transitioned from research to operation, we must recognize the critical importance of maintaining such a team effort to ensure the precision and stability of the measurement into the future.

Combined data from multiple altimeters have enabled a wide range of advances in ocean dynamics. Further, the combination with surface drifter data has led to the most detailed knowledge of the global ocean general circulation, revealing the unexpected ubiquitous presence of small-scale striations in ocean currents. It is now possible to conduct detailed analysis of the balance of vorticity, a high-order computation, of large-scale ocean currents. For the first time, one can track the movement of ocean eddies around the world's oceans and determine their pathways and interaction with mean circulation and ocean topography. The analysis of the balance of

energy in spectral space has led to a surprising finding of inverse cascade of energy associated with the first baroclinic mode of the ocean.

The specific orbit choice of T/P and its follow-ons has led to the most accurate knowledge of the surface (or barotropic) tides in the open ocean. The calculation of the energy flux of the tides proves that half of the energy required to mix ocean waters to maintain the large-scale thermohaline circulation comes from tidal dissipation in the deep ocean. The finding of internal tides in altimetry data is another surprise that creates a new surge of studies of the subject of fundamental importance in ocean mixing and tidal energy cycle.

A limitation of the conventional nadir-looking altimeter is its sampling in space and time. With data merged from two altimeters, the decade-long data set that has made great strides in advancing our knowledge of ocean circulation has a spatial resolution that prevents observation of the important sub-mesoscale processes at scales shorter than 100 km. A way to advance the capability of future altimetry is the use of radar interferometry for making high-resolution wide-swath altimetry measurement. The SWOT Mission recommended by the US National Research Council's Decadal Survey is taking on this challenge by developing a Ka-band radar interferometry system for flight in the late 2010s. SWOT measurement will significantly advance both oceanography and land hydrology and address two key aspects of climate change: improving the prediction of the rate of warming through improved understanding of the oceanic submesoscale processes, and improving the capability of monitoring and managing the shifting water resources caused by a warming climate.

By providing wide-swath coverage, a single mission like SWOT is equivalent to more than 10 conventional nadir-looking altimeters. After the demonstration of its workings, radar interferometry is potentially a candidate for replacing nadir-looking altimetry as a standard tool for oceanographic and hydrological applications.

Acknowledgements The research presented in the paper was carried out at the Jet Propulsion Laboratory, California Institute of Technology, under contract with the National Aeronautic and Space Administration. Support from the Jason-1 and OSTM/Jason-2 Projects is acknowledged.

References

Ablain M, Cazenave A, Valladeau G, Guinehut S (2009) A new assessment of the error budget of global mean sea level rate estimated by satellite altimetry over 1993–2008. Ocean Sci 5: 193–201

Alsdorf D, Fu LL, Mognard N, Cazenave A, Rodriguez E, Chelton D, Lettenmaier D (2007) Measuring the global oceans and terrestrial fresh water fromspace. EOS Trans AGU 88(24):253

Bamber JL, Riva REM, Vermeersen BLA, LeBrocq AM (2009) Reassessment of the potential sea-level rise from a collapse of the West Antarctic ice sheet. Science 324:901–903, doi:10.1126/science.1169335

Carrère L, Lyard F (2003) Modeling the barotropic response of the global ocean to atmospheric wind and pressure forcing – comparisons with observations. Geophys Res Lett 30:1275, doi:10.1029/2002GL016473

Cazenave A, Nerem RS (2004) Present-day sea level change: observations and causes. Rev Geophys 42:RG3001, doi:10.1029/2003RG000139

Chao Y, Fu LL (1995) A comparison between the TOPEX/POSEIDON data and a global ocean general circulation model during 1992–1993. J Geophys Res 100:24965–24976
Chelton DB, Schlax MG (1996) Global observations of oceanic Rossby waves. Science 272: 234–238
Chelton DB, Schlax MG (2003) The accuracies of smoothed sea surface height fields constructed from tandem satellite altimeter datasets. J Atmos Ocean Tech 20:1276–1302
Chelton DB, Schlax MG, Samelson RM, de Szoeke RA (2007) Global observations of large oceanic eddies. Geophys Res Lett 34:L15606, doi:10.1029/2007GL030812
de Miranda AP, Barnier B, Dewar WK (1999) On the dynamics of the Zapiola Anticyclone. J Geophys Res 104:21137–21150
Ducet N, Le Traon PY, Reverdin G (2000) Global high resolution mapping of ocean circulation from the combination of TOPEX/POSEIDON and ERS-1/2. J Geophys Res 105: 19477–19498
Egbert GD, Ray RD (2000) Significant dissipation of tidal energy in the deep ocean inferred from satellite altimeter data. Nature 405:775–778
Fu LL (2003) Wind-forced intraseasonal sea level variability of the extratropical oceans. J Phys Oceanogr 33:436–449
Fu LL (2004) Latitudinal and frequency characteristics of the westward propagation of large-scale oceanic variability. J Phys Oceanogr 34:1907–1921
Fu LL (2006) Pathways of eddies in the South Atlantic revealed from satellite altimeter observations. Geophys Res Letts 33:L14610, doi:10.1029/2006GL026245
Fu LL (2007) Intraseasonal basin modes of the equatorial Indian Ocean observed from sea surface height, wind, and temperature data. J Phys Oceanogr 37:188–202
Fu LL (2009) Pattern and velocity of propagation of the global ocean eddy variability. J Geophys Res 114:C11017, doi:10.1029/2009JC005349
Fu LL, Cazenave A (eds.) (2001) Satellite Altimetry and Earth Sciences: A Handbook of Techniques and Applications, Academic Press, San Diego, 463 pp
Fu LL, Chelton DB (2001) Large-scale ocean circulation. In: Fu LL, Cazenave A (eds.) Satellite Altimetry and Earth Sciences: A Handbook for Techniques and Applications, Academic Press, San Diego, pp. 133–169, 423pp
Fu LL, Cheng B, Qiu B (2001) 25-Day period large-scale oscillations in the Argentine Basin revealed by the TOPEX/POSEIDON altimeter. J Phys Oceogr 31:506–517
Fu LL, Ferrari R (2008) Observing oceanic submesoscale processes from space. Eos Trans AGU 89(48):488
Fu LL, Flierl GR (1980) Nonlinear energy and enstrophy transfers in a realistically stratified ocean. Dyn Atmos Ocean 4:2l9–246
Fu LL, Rodriguez R (2004) High-resolution measurement of ocean surface topography by radar interferometry for oceanographic and geophysical applications. In: Sparks RSJ, Hawkesworth CJ (eds.) State of the Planet: Frontiers and Challenges, AGU Geophysical Monograph 150, IUGG 19:209–224
Fu LL, Smith RD (1996) Global ocean circulation from satellite altimetry and high-resolution computer simulation. Bull Amer Meteorol Soc 77:2625–2636
Fukumori I, Raghunath R, Fu LL (1998) The nature of global large-scale sea level variability in relation to atmospheric forcing: a modeling study. J Geophys Res 103: 5493–5512
Hakkinen S, Rhines P (2004) Decline of subpolar North Atlantic circulation during the 1990s. Science 304:555–559, doi:10.1126/science.1094917
Huang NE, Leitao CD, Para CG (1978) Large-scale Gulf Stream frontal study using GEOS3 radar altimeter data. J Geophys Res 83:4673–4682
Hughes CW (2005) Nonlinear vorticity balance of the Antarctic Circumpolar Current. J Geophys Res 110:C1108, doi:10.1029/2004JC002753
Isern-Fontanet J, Garcia-Ladona E, Font J (2006) Vortices of the Mediterranean Sea: an altimetric perspective. J Phys Oceanogr 36:87–103, doi:10.1175/JPO2826.1
Isoguchi O, Kawamura H (2006) Seasonal to interannual variations of the western boundary current of the subarctic North Pacific by a combination of the altimeter and tide gauge sea levels. J Geophys Res 111:C04013, doi:10.1029/2005JC003080

Klein P, Isern-Fontanet J, Lapeyre G, Roullet G, Danioux E, Chapron B, Le Gentil S, Sasaki H (2009) Diagnosis of vertical velocities in the upper ocean from high resolution sea surface height. Geophys Res Lett 36:L12603, doi:10.1029/2009GL038359

Lapeyre G, Klein P (2006) Impact of the small-scale elongated filaments on the oceanic vertical pump. J Mar Res 64:835–851

Lee T (2004) Decadal weakening of the shallow overturning circulation in the South Indian Ocean. Geophys Res Lett 31:L18305, doi:10.1029/2004GL020884

Lee T, McPhaden MJ (2008) Decadal phase change in large-scale sea level and winds in the Indo-Pacific region at the end of the 20th century. Geophys Res Lett 35:L01605, doi:10.1029/2007GL032419

Le Provost C (2001) Ocean tides. In: Fu LL, Cazenave A (eds.) Satellite Altimetry and Earth Sciences: A Handbook for Techniques and Applications, Academic Press, San Diego, pp. 267–301, 423 pp

Le Traon PY, Morrow R (2001) Ocean currents and eddies. In: Fu LL, Cazenave A (eds.) Satellite Altimetry and Earth Sciences: A Handbook for Techniques and Applications, Academic Press, San Diego, pp. 171–210, 423 pp

Leuliette EW, Miller L (2009) Closing the sea level rise budget with altimetry, Argo, and GRACE. Geophys Res Lett 36:L04608, doi:10.1029/2008GL036010

Maximenko NA, Bang B, Sasaki H (2005) Observational evidence of alternating zonal jets in the world ocean. Geophys Res Lett 32:L12607, doi:10.1029/2005GL022728

Maximenko NA, Melnichenko OV, Niiler PP, Sasaki H (2008) Stationary mesoscale jet-like features in the ocean. Geophys Res Lett 35:L08603, doi:10.1029/2008GL033267

Merrifield MA, Holloway P, Johnston T (2001) The generation of internal tides at the Hawaiian Ridge. Geophys Res Let 28:559–562

Merrifield MA, Merrifield ST, Mitchum GT (2009) An anomalous recent acceleration of global sea level rise. J Climate 22:5772–5781

Morrow R, Florence B, Griffin D, Sudre J (2004) Divergent pathways of cyclonic and anti-cyclonic ocean eddies. Geophys Res Lett 31:L24311, doi:10.1029/2004GL020974

Munk WH, Wunsch C (1998) Abyssal recipes II: energetics of tidal and wind mixing. Deep Sea Res 45:1977–2010

Niiler PP, Maximenko NA, McWilliams JC (2003) Dynamically balanced absolute sea level of the global ocean derived from near-surface current. J Geophys Res 110:C11008, doi:10.1029/2004JC002753

Palacios DM, Bograd SJ (2005) A census of Tehuantepec and Papagayo eddies in the northeastern tropical Pacific. Geophys Res Lett 32:L23606, doi:10.1029/2005GL024324

Qiu B, Chen S (2010) Eddy-mean flow interaction in the decadally-modulating Kuroshio extension system. Deep Sea Res 57, doi:10.1016/j.dsr2.2008.11.036

Qiu B, Scott RB, Chen S (2008) Length scales of eddy generation and nonlinear evolution of the seasonally-modulated South Pacific Subtropical Countercurrent. J Phys Oceanogr 38: 1515–1528

Ray RD, Mitchum GT (1997) Surface manifestation of internal tides in the deep ocean: observations from altimetry and island gauges. Prog Oceanogr 40:135–162

Rhines PB (1977) The dynamics of unsteady currents. In: Goldberg E et al (eds.) The Sea, John Wiley and Sons, New York, pp. 189–318

Richards KJ, Maximenko NA, Bryan FO, Sasaki H (2006) Zonal jets in the Pacific Ocean. Geophys Res Lett 33:L03605, doi:10.1029/2005GL024645

Rio MH, Hernandez F (2004) A mean dynamic topography computed over the world ocean from altimetry, in situ measurements, and a geoid model. J Geophys Res 109:C12032, doi:10.1029/2003JC002226

Rodriguez E, Martin J (1992) Theory and design of interferometric synthetic aperture radars. IEEE Proc 139(2):147–159

Roemmich J, Gilson D, Davis R, Sutton P, Wijffels S, Riser S (2007) Decadal spinup of the South Pacific Subtropical Gyre. J Phys Oceanogr 37:162–173, doi:10.1175/JPO3004.1

Schlax MG, Chelton DB (2008) The influence of mesoscale eddies on the detection of quasi-zonal jets in the ocean. Geophys Res Lett 35:L24602, doi:10.1029/2008GL035998

Scott RB, Arbic BK (2007) Spectral energy fuxes in geostrophic turbulence: implications for ocean energetics. J Phys Oceanogr 37:673–688.

Scott RB, Wang F (2005) Direct evidence of an oceanic inverse kinetic energy cascade from satellite altimetry. J Phys Oceanogr 35:1650–1666

Stammer D, Tokmakian R, Semtner A, Wunsch C (1996) How well does a 1/4 degree global circulation model simulate large-scale oceanic observations? J Geophys Res 101:25779–25811

Stammer D, Wunsch C, Giering R, Eckert C, Heimbach P, Marotzke J, Adcroft A, Hill CN, Marshall J (2002) The global ocean circulation during 1992–1997, estimated from ocean observations and a general circulation model. J Geophys Res 107:3118, doi:10.1029/2001JC000888

Stammer D, Wunsch C, Ponte R (2000) De-aliasing of global high frequency barotropic motions in altimeter observations. Geophys Res Lett 27:1175–1178

Tapley BD, Bettadpur S, Ries JC, Thompson PF, Watkins MM (2004) GRACE measurements of massvariability in the earth system. Science 305:503–505, doi:10.1126/science.1099192

Weijer W, Viver F, Gille ST, Dijkstra H (2007) Multiple oscillatory modes of the Argentine Basin. Part I: Statistical analysis. J Phys Oceanogr 37:2855–2868

Wunsch C, Gaposchkin EM (1980) On using satellite altimetry to determine the general circulation of the oceans with application to geoid improvement. Rev Geophys Space Phys 18:725–745

Wunsch C, Heimbach P, Ponte RM, Fukumori I, ECCO-GODAE Consortium Members (2009) The global general circulation of the ocean estimated by the ECCO-Consortium. Oceanography 22:88–103